Dielectrophoretic liquid actuation and nanodroplet formation

T. B. Jones[a)]
Department of Electrical and Computer Engineering, University of Rochester, Rochester, New York 14627

M. Gunji and M. Washizu
Department of Mechanical Engineering, Kyoto University, Kyoto 606-8501, Japan

M. J. Feldman
Department of Electrical and Computer Engineering, University of Rochester, Rochester, New York 14627

(Received 20 July 2000; accepted for publication 20 October 2000)

Water, like any polarizable medium, responds to a nonuniform electric field by collecting preferentially in regions of maximum field intensity. This manifestation of dielectrophoresis (DEP) makes possible a variety of microelectromechanical liquid actuation schemes. In particular, we demonstrate a new class of high-speed DEP actuators, including ''wall-less'' flow structures, siphons, and nanodroplet dispensers that operate with water. Liquid in these microfluidic devices rests on a thin, insulating, polyimide layer that covers the coplanar electrodes. Microliter volumes of water, deposited on these substrates from a micropipette, are manipulated, transported, and subdivided into droplets as small as ~7 nl by sequences of voltage application and appropriate changes of electrode connections. The finite conductivity of the water and the capacitance of the dielectric layer covering the electrodes necessitate use of rf voltage above ~60 kHz. A simple RC circuit model explains this frequency-dependent behavior. DEP actuation of small water volumes is very fast. We observe droplet formation in less than 0.1 s and transient, voltage-driven movement of water fingers at speeds exceeding 5 cm/s. Such speed suggests that actuation can be accomplished using preprogrammed, short applications of the rf voltage to minimize Joule heating. © *2001 American Institute of Physics.* [DOI: 10.1063/1.1332799]

I. INTRODUCTION

Nonuniform electric fields exert a dielectrophoretic (DEP) force on polarizable media, including liquids such as water. With properly designed electrodes, the DEP effect may be exploited to control and manipulate small water volumes. In this article, we report voltage-controlled actuation of water, including manipulation of submicroliter volumes and dispensing of multiple nanodroplets, all accomplished on a chip using simple, coplanar electrodes. DEP actuation of water requires high frequency electric fields, and we present a simple model to explain this requirement.

In the past, exploiting DEP to manipulate aqueous media has been largely dismissed as impractical, due to the conductivity of water and the resultant, excessive Joule heating; however, the governing electromechanical and thermophysical laws scale in such a way as to create an opportunity for aqueous DEP on the microscale. Micro-DEP benefits from reducing electrode dimensions in a way analogous to the advantage gained by electrostatic forces in microelectromechanical systems (MEMS). Of equal importance in the case of water, reduced structure size also ameliorates Joule heating. The consequence of these scaling-law-derived advantages is the possibility of a new class of microfluidic systems based on droplets resting on a substrate. In the systems we envision, very short ($\leqslant$0.1 s) rf voltage applications and appropriate changes to the electrode connections are employed to actuate small volumes of water, moving them about on a substrate and dividing them into very small droplets for processing, mixing, separations, etc.

Major research effort is now being devoted to the integration of microfluidic systems with appropriate sensors and analytical components to create the ''laboratory on a chip.'' [1] Tools for chemical analysis such as capillary electrophoresis,[2] liquid chromatography,[3] and flow injection analysis[4] have been demonstrated on the microscale, and now attention is turning to automated, programmable systems for microassay. The defining feature of microassay is the use of very small inventories of substances, usually liquids or bioparticles suspended in aqueous media for testing and analysis. The liquids might be dangerous chemical substances or aqueous suspensions containing pathogens or rare and difficult to isolate disease-fighting cells. Advantages of microassay include reduced waste, faster reaction times, statistically more reliable results (because large numbers of individual tests can be conducted simultaneously), and full automation; however, the technical problems to be surmounted are considerable.

II. BACKGROUND

At the present time, most microfluidic schemes for the manipulation of small liquid volumes are enclosed systems of very small channels and the pumps, plenums, valves, and other components required to induce and then regulate flow through them. Cross-sectional dimensions range from ~1 to 100 μm (10^{-6}–10^{-4} m), requiring pressure heads up to

[a)]Author to whom correspondence should be addressed; electronic mail: jones@ece.rochester.edu

$\sim 10^4$ Pa to achieve usable flows. Fabrication of complex, reliably leak-free microstructures is a serious technical challenge. In addition, unavoidable shear flow and diffusion in tiny channels makes it difficult to eliminate intersample mixing and dead volumes.

Alternatives to such closed-channel systems are open structures, where small liquid masses, residing on a substrate, are divided, moved about, and configured by some controllable field of force. For example, a microliter-sized liquid volume, deposited by conventional means on the surface, might be divided into a large number of discrete droplets for subsequent mixing, combinatorial reacting, assay, or other operations. Dividing an initial liquid inventory into discrete droplets (nanoliter or smaller) greatly reduces the risk of inadvertent intersample mixing and contamination. Furthermore, by sealing the entire chip and controlling vapor pressure within the enclosure, 100% utilization of samples and reagents might be realized. Integration of open structures with any required control electronics, position sensors, and diagnostic components should present few technical difficulties.

Direct electrical actuation mechanisms for closed-channel, microfluidic systems include ion-drag pumping, electroconvection, and electro-osmosis. Ion-drag pumps commonly require dc potentials of the order of 10^3 V but consume very little power.[5] Somewhat related to these are electro-osmotic devices, one example being an electrochemically actuated pump that operates analogous to a field-effect transistor.[6] Electro-osmotically driven flow utilizing chemically patterned structures also has been investigated.[7]

To achieve controllable flow in open structures, a range of phenomena are under investigation.[8] For example, Gau *et al.* reported capillary phenomena for passive control of liquid using substrates patterned with hydrophobic and hydrophilic areas.[9] Gallardo *et al.* employed a two-dimensional array of individually addressable electrodes to harness a voltage-controlled, reversible electrochemical reaction that creates or consumes surfactant agent and thereby establishes surface-tension-gradient-driven fluid motion.[10] Ichimura *et al.* have used a photoresponsive surface to induce droplet motion by an imbalance of the contact angle from one side to the other of a droplet.[11] Another effect, thermocapillarity, exploits the temperature dependence of surface tension to induce flow.[12]

In contrast to the above, DEP liquid actuation relies on coplanar electrodes patterned on a smooth, insulating substrate, and then covered by a thin dielectric layer. Liquid masses resting on the substrate are manipulated, transported about, and divided into nanodroplets by programmed sequences of rf voltage application and appropriate changes to the electrode connections. Subsequent droplet transport, mixing, and separation should be possible by integrating DEP liquid actuation with Washizu's droplet transport scheme.[13] His scheme uses low-frequency ac voltage (50 Hz) applied to an array of parallel strips covered by a thin dielectric layer and arranged like railroad ties, that is, perpendicular to the intended direction of travel. By sequential application of voltage to the electrodes lying almost directly underneath but only on one side, the droplet can be moved in either direction. If this scheme can be combined with DEP actuation, a ''nanodroplet switchyard'' might be envisioned.

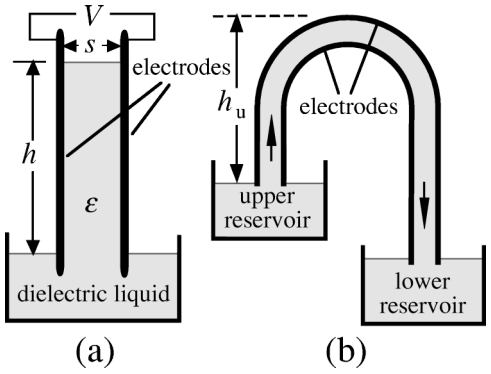

FIG. 1. Dielectrophoresis of insulating dielectric liquids. (a) Pellat's original experiment (Ref. 19). (b) The dielectric siphon experiment (Ref. 20).

III. LIQUID DIELECTROPHORESIS

Pohl originally defined dielectrophoresis as the attraction of uncharged but polarizable particles into regions of higher electric field intensity.[14] DEP liquid actuation is not concerned with particles inside the liquid. Rather, it exploits the force to manipulate liquid masses. Liquid DEP is phenomenologically similar to particulate DEP in that polarizable liquids also are drawn into regions of stronger electric field intensity, but there is the additional manifestation that the electric field also influences the shape. Unlike other electrohydrodynamic (EHD) effects such as ion drag, liquid DEP is not, strictly speaking, a pumping mechanism. Instead, like capillarity, it creates new hydrostatic equilibria, which may be exploited to contain liquids in ''wall-less'' flow structures.[15,16] The nonuniform electric field provides this containment, much like gravity holds water in a ditch or the capillary force confines kerosene in a lamp wick. At one time, the U.S. space program considered exploiting liquid DEP in zero-gravity applications such as spacecraft fuel tanks[17] and heat pipes.[18]

A. Wall-less flow structures and siphons

Pellat's classic demonstration of the ponderomotive force on liquids provides a basis for understanding wall-less flow structures[19] [see Fig. 1(a)]. Two plane, parallel electrodes, oriented vertically and at spacing s, are partially immersed in a pool of dielectric liquid of mass density ρ, and dielectric permittivity ϵ. The liquid is covered by a gas of mass density negligible compared to the liquid and permeability equal to free space, $\epsilon_0 = 8.854 \times 10^{-12}$ F/m. When voltage V is applied to the electrodes, the liquid between the electrodes rises to a static height h:[15,16]

$$h \approx \frac{(\epsilon - \epsilon_0) V^2}{2 s^2 \rho g}. \tag{1}$$

In Eq. (1), $g = 9.81\ \mathrm{m/s^2}$ is the terrestrial acceleration due to gravity.

A good example of a wall-less flow structure is the dielectric siphon,[20] which is a simple modification of Pellat's experiment consisting of two closely spaced electrodes run-

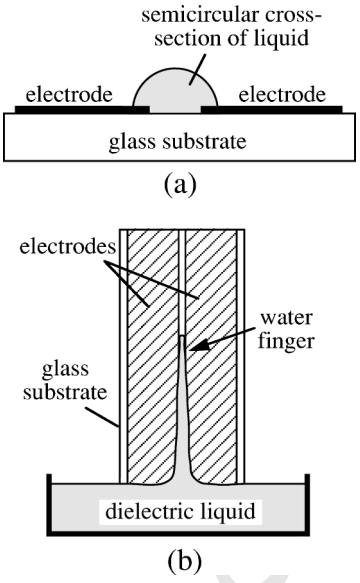

FIG. 2. Planar electrode configurations for wall-less flow structures. Sketches are not to scale. (a) Cross section of original microelectrode structure used with insulating transformer oil. The liquid forms a semicircular profile centered on the gap. (b) Side view of dielectric height-of-rise experiment showing liquid finger extending upward in the gap between the coplanar electrodes.

ning between an upper and a lower reservoir [see Fig. 1(b)]. The DEP force confines dielectric liquid between the electrodes. If the voltage is sufficiently high, that is, if $V \geqslant V_{\min}$, where

$$V_{\min} = \sqrt{2\rho g h_u s^2/(\epsilon - \epsilon_0)} \tag{2}$$

and h_u is the vertical distance between the upper reservoir's liquid surface and the highest point of the siphon, fluid communication is established between the upper and lower reservoirs and the net gravitational head induces flow. If the voltage V is reduced below $V_{\min}$, liquid drains from the top and siphon action ceases.

B. DEP microfluidics with dielectric liquid

Flow structures with electrodes at millimeter spacings require voltages in excess of ~20 kV and electric field intensities, $E = \mathrm{V/s}$, that exceed air breakdown. To avoid breakdown, pressurization to $\sim 10^6$ Pa (~10 atm) has been used.[20] In an attempt to circumvent the high-voltage requirement, a bench-top experiment without pressurization was performed using miniaturized electrodes fabricated from vapor-deposited Al-on-glass.[21] [see Figs. 2(a) and 2(b)]. Using highly insulating transformer oil ($\epsilon/\epsilon_0 \approx 2.4$, $\rho \approx 900\ \mathrm{kg/m^3}$) and voltage $V \approx 200$ V rms at 60 Hz ac, a narrow finger of liquid is observed to rise between the electrodes, eventually reaching a height of several centimeters. The finger, thicker at the bottom than at the top, has a semicircular cross section centered on the gap. Upon removal of the voltage, the liquid drains very slowly, leaving behind a thin film.

Electrical breakdown is avoided in this experiment because the reduced electrode size exploits the favorable scaling law for liquid dielectrophoresis.[22] This law is exemplified as follows: If an electrode structure is scaled down by some factor $\alpha < 1$, then the voltage required to maintain the DEP force per unit volume at some fixed value goes down as $\alpha^{3/2}$ and the electric field strength goes down as $\alpha^{1/2}$. Therefore, reducing structure size simultaneously addresses the problems of excessive voltage requirement and electrical breakdown.

C. Microdielectrophoretic actuation of water

At least in terrestrial gravity, the intense electric fields associated with centimeter-scale electrode structures would seem to preclude DEP manipulation of water because of Joule heating and electrolysis. The heating is excessive even for distilled or deionized water, which has electrical conductivity σ_w in the range of 10^{-4}–10^{-5} S/m. Fortunately, two factors intervene when DEP actuation is considered for microfluidic applications. First, the thermophysical scaling laws reduce heating by enhancing conductive heat transfer. This point is discussed in a later section of the article. Second, we find that the exposure time of the water to the electric field can be kept to a minimum, thanks to the very rapid response of submicroliter water volumes to DEP actuation. The strategy is to apply the rf voltage for a time just sufficient to actuate the desired liquid movement, and then to remove it immediately. In this respect, DEP actuation of water is distinct from previous experiments, where hydrostatic equilibria were attained with *insulating* dielectric liquids using very high field strengths.[15–18,20] In the present case, the same dielectrophoretic phenomena are enlisted; however, actuation is the transient, electromechanical response of a liquid mass seeking the new equilibrium imposed by the nonuniform electric field. The voltage is removed as soon as the desired new equilibrium, e.g., the distribution of liquid throughout a network of reservoirs or formation of nanodroplets has been attained.

The first tested with water was the simple flow structure depicted in Fig. 3(a). The only difference from Fig. 2(a) is the ~10 μm (10^{-5} m) spin coated, polyimide layer that covers the planar electrodes. This layer prevents electrolysis and blocks any dc or low-frequency component of current in the water. The liquid DEP effect is strongly dependent on frequency f. For $f \geqslant 60$ kHz, water accumulates in the compact, semicircular cross section of Fig. 3(a). On the other hand, at $f \approx 30$ kHz, the water spreads slowly in a thin layer as shown in Fig. 3(b) and, for $f \leqslant \sim 10$ kHz, the electric field has no apparent influence at all. This frequency dependence is one feature distinguishing liquid DEP, an electromechanical effect, from electrowetting; a term used to describe how a voltage applied between a conductive liquid mass and a conductive, but insulation-coated substrate alters effective contact angle.[23] In our experiment, the water is not an equipotential body. While electrowetting may influence initial formation of the water finger, it has no effect on the liquid profile.

Figure 4 shows a sequence of video micrographs of a flow structure in operation. The two electrode strips, photolithographically patterned in Al on glass substrates, have width $w \approx 1$ mm (10^{-3} m), operating length $L \approx 3$ cm (3×10^{-2} m), and spacing $g \approx 100\ \mu$m (10^{-4} m). The polyim-

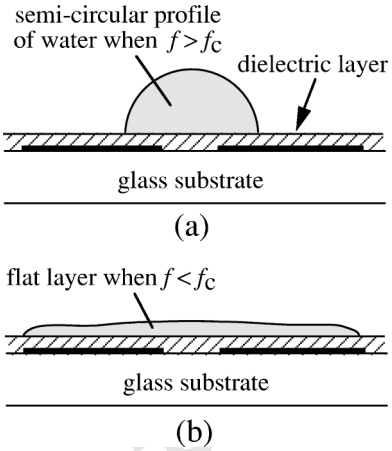

FIG. 3. DEP ''wall-less'' microstructures using water. Note the thin, insulating dielectric layer that covers the electrodes. Sketches are not to scale. (a) Cross section of present experimental configuration using water and dielectric-coated electrodes. The compact, semicircular profile shown here is observed for $f \geqslant \sim 6\times10^4$ Hz. (b) Liquid profile observed for $f=3\times10^4$ Hz. With horizontal electrodes, the water spreads out to cover the electrodes but moves only a short distance along the axis of the structure.

ide layer has thickness $t \approx 10\,\mu$m and dielectric permittivity $\epsilon_d \approx 3\epsilon_0$. In the experiment shown, a ~10 microliter droplet was deposited on the substrate with a micropipette and then voltage at $\sim 10^5$ Hz was turned up by hand to ~700 V rms. A narrow liquid finger projects from the droplet and moves along the gap, turning the two 90° corners before reaching the end of the structure. When the voltage is rapidly applied with a switch or relay, the finger forms and travels the ~3 cm length of the structure in less than ~0.2 s. Based on the volume of liquid reaching the far end of the structure and the lapsed time, one may estimate the transient flow rate at ~1 microliter per second ($\sim 10^{-9}$ m^3/s).

D. Frequency-dependence of liquid profile

The frequency dependence of the liquid profile is due to the capacitive coupling of the planar electrodes to the water, which has finite conductivity. An estimate for the critical frequency f_c separating the high- and low-frequency regimes depicted in Figs. 3(a) and 3(b) may be determined by reference to the RC circuit model in Fig. 5(a). The two series capacitors, C_d, represent the dielectric coating, while the conductance G_w and capacitance C_w model ohmic conduction and capacitance in the water, respectively. Figure 5(b) defines the physical parameters needed for computation of the circuit values, including the overlap δw, which can only be estimated from examination of the micrographs:

$$C_d \approx \frac{\epsilon \delta w L}{t} \tag{3a}$$

$$G_w \approx \frac{\sigma_w K(1-k^2)L}{2K(k^2)} \quad \text{and} \quad C_w \approx \frac{\epsilon_w}{\sigma_w} G_w \tag{3b}$$

K is the complete elliptical integral of the first kind with argument $k^2=[g/(g+2\,\delta w)]^2$, while σ_w and ϵ_w are the conductivity and dielectric permittivity of the water, respectively. The expression for G_w is exact for the conductance

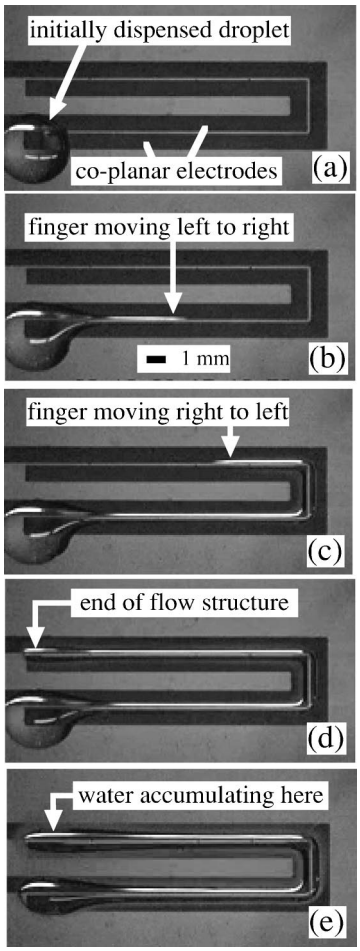

FIG. 4. Sequence of videomicrographs of horizontally mounted ''wall-less'' flow structure operating with water of electrical conductivity $\sigma_w \approx 10^{-4}$ S/m. The electrode gap is ~100 μm and the rf voltage ($\sim 10^5$ Hz) is turned up by hand over a period of several seconds to ~700 V rms. (a) Voltage off: ~10 ml droplet dispensed by micropipette at lower left; (b) voltage on: finger starting to extend to right along flow structure; (c) voltage on: water finger has rounded two 90 ° turns; (d) voltage on: water finger has reached end of structure; (e) voltage on: water is now accumulating at end of structure (upper left).

between two very thin, parallel, and coplanar strips of length L, width δw, and spacing g, lying on the lower boundary of a semi-infinite half-space of conductivity σ_w.[24] Because the water occupies only a semicircular column of radius ($g/2+\delta w$) centered on the midpoint of the gap, Eq. (3b) underestimates G_w but any error is overwhelmed by uncertainty in the value of σ_w. The critical frequency is

$$f_c = \frac{G_w}{2\pi(C_d/2+C_w)}. \tag{4}$$

For frequency $f \ll f_c$, virtually the entire voltage drop occurs across the dielectric layer and the water becomes an equipotential body. With zero electric field in the water, there is no significant DEP force acting to shape its profile. In the regime depicted by Fig. 3(b), electrowetting may be in force, but it is not effective in guiding water along the axis of the flow structure. In the high frequency regime, defined by f

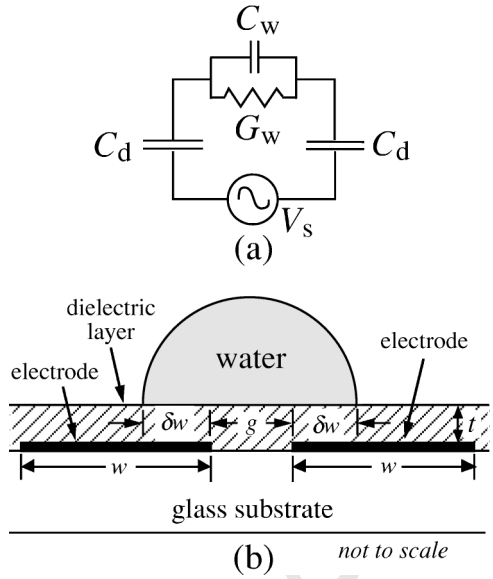

FIG. 5. Circuit model and cross section of flow structure. At high frequency (i.e., $f \gg f_c$), voltage drops across the bulk of the water, thus establishing the strong, nonuniform electric field that collects liquid in compact semicircular profile. (a) RC circuit model for the DEP actuator. (b) Semicircular cross section of liquid-filled flow structure for computation of circuit parameters. Sketch is not to scale.

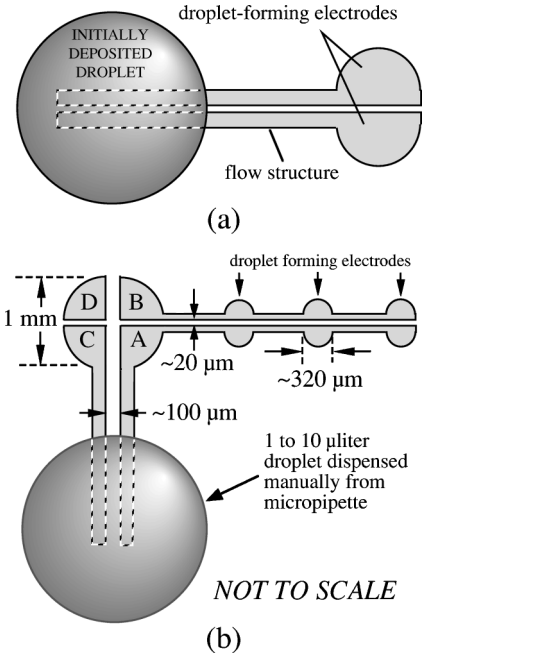

FIG. 6. Coplanar electrode configurations for droplet formation (not shown to scale). (a) Basic structure for droplet formation using bisected circular electrodes; (b) two-stage droplet formation structure. To fill intermediate reservoir from large droplet, electrodes A and B are connected together, as are C and D. After the reservoir is filled, A is connected to C and B is connected to D for droplet formation.

$\gg f_c$, some portion V_w of the total applied voltage V_s occurs in the water. This fraction is determined by capacitive voltage division.

$$\frac{V_w}{V_s} = \frac{C_d/2}{C_d/2 + C_w}. \tag{5}$$

Using $\epsilon_d/\epsilon_0 \approx 3$, $\epsilon_w/\epsilon_0 \approx 80$, $\sigma_w \approx 10^{-4}$ S/m, and $\delta w \approx 100\,\mu$m, one obtains: $G_w \approx 2\times10^{-6}$ S, $C_w \approx 14\times10^{-12}$ F, and $C_d \approx 8\times10^{-12}$ F. Then, from Eq. (4), $f_c \approx 20$ kHz, which is consistent with the transition we observe near 30 kHz. Using these circuit values in Eq. (5) yields the result that only ~20% of the voltage $V_s = 700$ V rms is applied to the water. This percentage is apparently sufficient to create the compact, semicircular profile of Fig. 3(a).

We have conducted no experimental investigation of the liquid profile using conductivity as a variable; however, because $f_c \propto \sigma_w$, studying the dependence of the liquid profile on frequency provides essentially equivalent information. Note that frequency-conductivity scaling applies to the cross-sectional profile of the water, but not to Joule heating, which is discussed in a later section.

IV. NANOLITER DROPLET FORMATION

A simple modification of the basic coplanar electrode structure facilitates DEP-actuated formation of multiple water droplets. Figure 6(a) shows a flow structure terminated by a bisected circle. A large droplet is deposited at the opposite end of the structure and voltage is applied. When the liquid finger reaches the circular area, the water rapidly spreads and covers the entire circular area, forming a well-defined hemispherical droplet. When voltage is turned off, the DEP force stabilizing the liquid in the flow structure is removed and the capillary jet instability pinches off the water.[25] Within less than 1/30 s, the water contained in the flow structure is gathered into the mass on the circular electrodes.

We used the two-stage droplet generator shown in Fig. 6(b) as a more realistic test of the droplet formation scheme. Note the four, individually addressable electrode sections: A, B, C, and D. The larger circular electrode at the upper left, 1 mm in diameter and divided into four quadrants, functions as an intermediate reservoir. In line and to its immediate right are three, bisected droplet formation electrodes (~320 μm in diameter). In operation, a large droplet (at lower right) is deposited manually with a micropipette. The initial position of this droplet is not critical, as long as it sits atop the flow structure. With electrode A connected to B, and C connected to D, a voltage of ~700 V rms at ~100 kHz is momentarily applied. In response, a finger of water projects from the large droplet, moving very rapidly along the 100 μm gap and filling the intermediate reservoir [see Figs. 7(a) and 7(b)]. Examination of individual video frames reveals that this reservoir fills in $\leq$0.1 s. When the voltage is removed, the flow structure connecting the large droplet to the intermediate reservoir drains rapidly, leaving the isolated ~100 nl droplet shown in Fig. 7(c). Occasionally, a small satellite droplet is left stranded somewhere in the middle of the flow structure. Next, electrode A is connected to C, and B to D, and voltage at ~500 V rms is applied momentarily. Now, a finger projects from the intermediate droplet, moving from left to right along the 20 μm gap and filling the three, small, circular electrodes, again in $\leq$0.1 s [see Fig. 7(d)]. With voltage

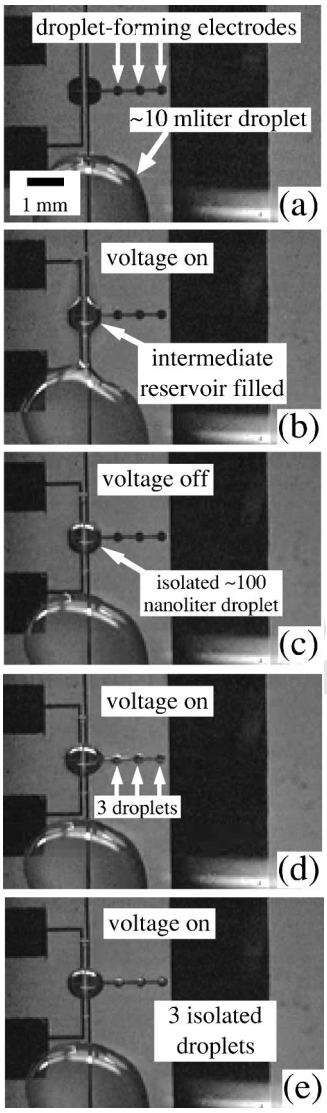

FIG. 7. Sequence of videomicrographs of droplet-formation electrode structure in operation with water of electrical conductivity $\sigma_w \approx 10^{-4}$ S/m and rf voltage at $\sim 10^5$ Hz. (a) Voltage off: ~10 ml droplet dispensed by micropipette is at lower left. (b) voltage on: ~100 nl reservoir has filled with water from large droplet; (c) voltage off: electrode connections are now switched for droplet formation; (d) voltage on: three droplets have formed in line to the right-hand side of intermediate reservoir; (e) voltage off: three isolated droplets of volumes ~8, ~7, and ~6 nl have formed.

removed once again, all connecting flow structures drain, leaving an isolated droplet atop each of the circular electrodes as shown in Fig. 7(e).

Each of the droplets assumes an approximately hemispherical shape, facilitating estimates of droplet volumes from the measured diameters [from left to right in Fig. 7(e)] these volumes are approximately 8, 7, and 6 nl (all ± 1 nl), respectively. The most likely explanation for this variation is differences in the locations of the capillary pinchoff points after voltage removal. In fact, the liquid volume contained within each of the interconnecting structures is ~1 nl. Note also that the electrode on the far right-hand side is connected to the flow structure on only one side. Our video camera does not provide sufficient temporal resolution to determine where capillary pinchoffs occur.

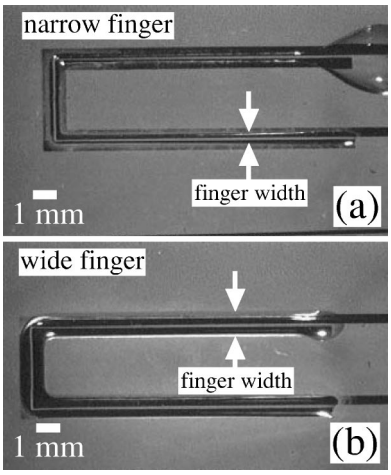

FIG. 8. Indeterminancy of liquid configuration for coplanar electrodes: width $w = 500\ \mu$m; gap spacing $g = 100\ \mu$m; polyimide layer $t = 10\ \mu$m. Both experiments conducted at $V_s \sim 700$ V and $f = 100$ kHz. (a) Narrow water finger confined to vicinity of gap; (b) wide water finger spanning entire width of electrode structure.

V. DISCUSSION

The rapid, field-induced movement of the liquid finger and the speed at which droplets form are unexpected and not consistent with the earlier micro DEP experiments using transformer oil.[21] The lower viscosity of water certainly has some influence, but wetting may be more important. The contact angle for water on polyimide is between 70° and 80°. We observe that, when the surface wetting is altered by rf breakdown, movement of the finger becomes sluggish. Furthermore, when the polyimide layer is coated with amorphous Teflon (with contact angle ~105°), DEP microactuation does not occur.

That water always seems to fill the entire circular area of the droplet-forming electrodes might seem inconsistent with Fig. 4, where the water confines itself to the region of the gap. Because a fuller understanding of how dielectrophoresis, surface tension, and surface wetting interact to form droplets is vital to optimization of DEP liquid actuation schemes, we performed additional experiments using electrode structures having fixed gap g but varied width w. The central finding is that, as structure aspect ratio w/g is decreased, a point is reached where the liquid profile can assume either of two distinct configurations, one with the finger confined to the gap and the other with the finger spanning the entire electrode structure. Figures 8(a) and 8(b) show video micrographs of experiments performed with two electrode structures of identical dimensions: $w = 500\ \mu$m and $g = 100\ \mu$m. Each experiment was videotaped and the frames shown are those where the water finger has just reached the end of the structure. Figure 8(a) shows the narrow configuration similar to Fig. 4, but in Fig. 8(b), the finger spans the entire structure.

We do not yet understand why identical electrodes exhibit this indeterminate behavior. One hypothesis is that the locally very strong electric field *directly over the edges of the electrodes* disrupts the liquid/solid contact, effectively puncturing the droplet surface to initiate finger formation. With

capillarity thus circumvented, the DEP force then draws the liquid forward in the finger. The plausibility of this theory rests on the intensification of the electric field near the very sharp inside and outside edges of the strips. Extending this hypothesis, one might postulate that the locally intense electric field pins the contact line directly over the electrode edges, in effect constraining the sides of the semicircular column. Therefore, once a finger, narrow or wide, has emerged from the parent droplet, its sides can be constrained along either the inner or the outer edges of the electrodes, respectively. As long as the voltage is on, this pinning presumably stabilizes the liquid against capillary instability.[25] This hypothesis, while consistent with our observations to date, needs to be further studied and tested.

A. Heating

In the past, excessive Joule heating has been thought to preclude practical application of the DEP force for manipulating aqueous media. In our work, heating was only evident in the initial experiment with the flow structure, because the voltage was turned up slowly by hand and the water was exposed to the rf field for several seconds. A buildup of condensate on the cool surface of the substrate immediately adjacent to the finger is faintly visible in Fig. 4(d). As predicted by the circuit model of Fig. 5(a) with water of conductivity $\sim 10^{-4}$ S/m, heating is pronounced only well above the critical frequency f_c.

DEP actuation of water having higher conductivity will require still higher electrical frequency. For cell media of conductivity $\sim 10^{-1}$ S/m, $\sim 10^{8}$ Hz may be needed. Furthermore, for fixed physical dimensions and voltage, Joule heating per unit volume increases directly with σ, so improved heat dissipation will be necessary. Fortunately, there are good prospects for circumvention of the heating problem. Perhaps most important is our finding that small water masses respond so quickly to an applied field. Having yet made no effort to optimize geometry, we nevertheless achieve flow rates exceeding ~ 1 microliter/s and finger movement in excess of 5 cm/s. These high speeds suggest the idea of a ''nanodroplet switchyard,'' that is, a droplet-based, DEP microfluidic system consisting of coated, coplanar microelectrodes, with all electrode connections and rf voltage applications fully automated and programmed. In such a system, the short voltage duty cycles would minimize heating in the liquid bulk.

Another way to control heating is to reduce structure size. Such a step, regarded as necessary anyway if subnanoliter droplet formation and manipulation are to be achieved, will benefit from the thermophysical scaling law governing heat rejection. Conduction into the substrate, the dominant heat dissipation mechanism, is proportional to contact area, while Joule heating is proportional to volume. Such surface-to-volume competition clearly favors smaller size. Furthermore, the previously mentioned scaling law for the DEP force also delivers a benefit from the standpoint of heating. In particular, if electrode size is scaled down by $\alpha < 1$, the electric field goes down by $\alpha^{1/2}$ and, because Joule heating is proportional to E^2, the heat *per unit volume* is reduced by α.

A third strategy to reduce heating is to fabricate the electrode arrays on materials of higher thermal conductivity. So far, we have used common glass substrates exclusively; however, other materials with better properties certainly exist. For example, crystalline quartz, an excellent electrical insulator, has thermal conductivity about a factor of 10 greater than glass, and silicon, though not highly insulating, has thermal conductivity a factor of 100 higher. Another possibility already showing promise in preliminary tests is to coat metallic (Al) substrates with a dielectric layer, pattern coplanar electrodes on this layer, and then apply the thin dielectric coat on top.

B. Electrical breakdown

Using the conductance and capacitance values calculated for the circuit model of Fig. 6(a) nearly 80% of the applied voltage $V_s = 700$ V rms is shared by the two capacitors C_d representing the dielectric layer. We estimate the electric field strength in this layer:

$$E_d = \frac{V_s - V_w}{2t} \approx 2.8 \times 10^7 \text{ V/m}. \tag{6}$$

An electric field strength of ~ 28 V per micron is close to the breakdown limit for polyimide, and it is probable that current-limited rf breakdown is occurring in the bulk of the polyimide layer. If so, the electric field strength in the water is actually higher than the simple linear theory would predict, enhancing the DEP effect.

rf surface discharges are sometimes observed in the gap between the coplanar electrodes; images recorded with an image intensifier camera reveal that such phenomena may be fairly common at the voltages now used. There might be a correlation between these discharges and localized alteration of the surface wetting properties of the polyimide. Often, substrates are found to work only one time. In subsequent tests, even after cleaning a damaged substrate with solvent and subsequent drying at high temperature, only a sluggish response to voltage is seen. In these cases, it appears that the polyimide surface has become more hydrophilic. Such behavior is no surprise; printing on plastic films routinely uses rf pretreatment to increase ink acceptance.

Vallet *et al.* report electrical discharge-induced changes in surface wetting for water droplets spreading on electrodes coated by dielectric layers.[26] They used voltage comparable to ours but at a lower frequency, ~ 1 kHz, where the droplet is effectively an equipotential and the electric field is limited to the dielectric layer. Because the water forms a very sharp edge along the contact line due to electrowetting, any discharge must occur there first. In contrast, the high-frequency discharges we observed occur along the inside edges of the electrodes, and are extinguished when the water finger arrives.

VI. CONCLUSION

For droplet volumes ranging from microliters down to nanoliters and planar microelectrodes with gaps from ~ 20 to ~ 100 μm, dielectrophoresis provides a controllable force for the manipulation of small water volumes, despite strong sur-

face tension and wetting phenomena. We have successfully exploited this force to move masses of water rapidly around a smooth substrate and to create multiple nanoliter droplets in less than ~0.1 s. Once formed, movement of these droplets across a substrate for diagnostics, mixing, separations, and dispensing, all under remote, programmable, electrical control should be achievable. There are interesting implications for such a capability in the ''laboratory on a chip.'' The foremost advantage is that division of an initial liquid inventory into discrete droplets before processing avoids sample cross contamination due to diffusion- and shear-flow related effects. Using a discrete sample could be very important in sensitive assay protocols and combinatorial chemistry. Other advantages include speed as well as the avoidance of problems associated with pump priming or, for liquids containing particulate matter such as cells, channel clogging. A further observation is that, because droplet-based systems should be fully compatible with closed channel systems, DEP liquid actuation might provide means for interfacing microfluidic channels with macrofluidic components.[27]

DEP liquid actuation on the microscale involves a complex interplay of phenomena: dielectrophoresis, capillarity and wetting, transient fluid dynamics, Joule heating, and rf discharge. Many questions are unanswered. The 1/30 second framing speed of our video camera has prevented us from yet determining upper limits for either transient liquid flow rates or the velocity of water fingers. Furthermore, we know neither the lower limit on droplet formation size nor the upper limit on electrical conductivity for effective DEP actuation of aqueous media. Major challenges to development of the droplet switchyard include amelioration of Joule heating, scaling down electrode structure sizes to facilitate subnanoliter droplet formation, and reduction of the required voltage. Reducing electrode size and reducing the thickness of the dielectric coating show promise in reduction of the voltage and elimination of rf discharges, but better dielectric coatings and fabrication methods to control surface wetting must be identified.

ACKNOWLEDGMENTS

One of the authors (T. B. J.) gratefully acknowledges long-term fellowship support from the Japan Society for the Promotion of Science and from the U.S. National Science Foundation (Center for Global Partnership). M. Gunji performed all experiments using water at Kyoto University.

[1] *Micro Total Analysis Systems '98*, edited by D. J. Harrison and A. Van Den Berg (Kluwer, Dordrecht, 1998).
[2] D. J. Harrison K. Fluri, Z. Fan, and K. Seiler, in *Micro Total Analysis Systems*, edited by A. Van Den Berg and P. Bergveld (Kluwer, Dordrecht, 1995), pp. 105–115.
[3] J. Manz, E. Verpoorte, D. E. Raymond, C. S. Effenhauser, N. Burggraf, and H. M. Widmer, in *Micro Total Analysis Systems*, edited by A. Van Den Berg and P. Bergveld (Kluwer, Dordrecht, 1995), pp. 5–27.
[4] J. Ruzicka, in *Micro Total Analysis Systems*, edited by A. Van Den Berg and P. Bergveld (Kluwer, Dordrecht, 1995), pp. 117–125.
[5] S. E. McBride, R. M. Moroney, and W. Chiang, in *Micro Total Analysis Systems '98*, edited by D. J. Harrison and A. Van Den Berg (Kluwer, Dordrecht, 1998), pp. 45–48.
[6] R. B. M. Schasfoort, S. Schlautmann, J. Hendrikse, and A. van den Berg, Science **286**, 942 (1999).
[7] A. D. Stoock, M. Weck, D. T. Chin, W. T. S. Chiu, T. S. Huck, P. J. A. Kenis, R. F. Ismagilov, and G. M. Whitesides, Phys. Rev. Lett. **84**, 3314 (2000).
[8] M. Grunze, Science **283**, 41 (1999).
[9] H. Gau, S. Herminghaus, P. Lenz, and R. Lipowsky, Science **283**, 46 (1999).
[10] B. S. Gallardo, V. K. Gupta, F. D. Eagerton, L. I. Jong, V. S. Craig, R. R. Shah, and N. L. Abbott, Science **283**, 57 (1999).
[11] K. Ichimura, S.-K. Oh, and M. Nakagawa, Science **288**, 1624 (2000).
[12] D. E. Kataoka and S. M. Troian, Nature (London) **402**, 794 (1999).
[13] M. Washizu, IEEE Trans. IAS **IAS-34**, 732 (1998).
[14] H. A. Pohl, J. Appl. Phys. **22**, 869 (1951).
[15] T. B. Jones and J. R. Melcher, Phys. Fluids **16**, 393 (1973).
[16] T. B. Jones, J. Appl. Phys. **45**, 1487 (1974).
[17] J. R. Melcher, D. S. Guttman, and M. Hurwitz, J. Spacecr. Rockets **6**, 25 (1969).
[18] T. B. Jones, Int. J. Heat Mass Transf. **16**, 1045 (1973).
[19] H. Pellat, C. R. Seances Acad. Sci. (Paris) **119**, 675 (1894).
[20] T. B. Jones, M. P. Perry, and J. R. Melcher, Science **174**, 1232 (1971).
[21] T. B. Jones (unpublished).
[22] A. S. Bahaj and A. G. Bailey, *Proc. IEEE/IAS Annual Meeting*, Cleveland, OH, 1979, pp. 154–157.
[23] J. A. M. Sondag-Huethorst and L. G. L. Fokkink, J. Electroanal. Chem. **367**, 49 (1994).
[24] W. R. Smythe, *Static and Dynamic Electricity*, 2nd ed. (McGraw-Hill, New York, 1950), pp. 100–102.
[25] S. Schiaffino and A. A. Sonin, J. Fluid Mech. **343**, 95 (1997).
[26] M. Vallet, M. Vallade, and B. Berge, Eur. Phys. J. B **11**, 583 (1999).
[27] D. J. Harrison, in *Micro Total Analysis Systems '98*, edited by D. J. Harrison and A. Van Den Berg (Kluwer, Dordrecht, 1998), p. (iii).